ADVANCED FUNCTIONAL MATERIALS
www.afm-journal.de

www.MaterialsViews.com

Nanostructured Hybrid Materials for the Selective Recovery and Enrichment of Rare Earth Elements

Justyna Florek, François Chalifour, François Bilodeau, Dominic Larivière, and Freddy Kleitz**

The importance of rare-earth elements (REEs) in the global economy is booming as they are used in numerous advanced technologies. Industrially, the extraction and purification of REEs involve multiple liquid–liquid extraction (LLE) steps as they exhibit very similar complexation properties with most common ligands. In order to substantially improve this process and provide a greener alternative to LLE, functional porous hybrid materials, demonstrating enhanced selectivity towards heavier REEs compared to commercially-available products, are proposed. In addition, because of the grafting procedure used in the synthesis, the proposed materials demonstrate a higher degree of reusability, increasing their marketable potential.

1. Introduction

Since the beginning of this millennium, the rare-earth elements (REEs) global consumption rate has increased significantly while supplies have drastically diminished, mainly as the result of restrictions on exportations from China. According to the latest market analyses, carried out by the USA and Chinese governments, the exploitation of REEs over the past few years remains constant, although the demand for rare-earth compounds has been growing rapidly worldwide.[1] High purity REEs have found applications in numerous advanced technologies, such as for the production of magnets, chemical sensors or lasers.[2,3] In domestic electronics, REEs are used in computers, plasma and LCD screens, cell phones or cameras. Among roughly 250 REE minerals that can be found, only 10–20 are considered as useful, while only 5 are practically applicable.[4] Therefore, the main objective of the present work is the development of efficient solid sorbents for the extraction and valorization of REEs, especially from alternative sources, e.g., industrial or mining wastes. Mining residues contain a number of elements, including some radioactive elements, transition metal oxides, as well as REEs, which often are present at economically interesting concentrations.[5] However, selective lanthanide separation and pre-concentration is one of the most difficult tasks, as these elements have only subtle differences in their properties.[6] Industrially, extraction and purification of REEs require multiple sequential extraction steps, which are mostly based on liquid-liquid or liquid-solid extraction procedures. Liquid–liquid extraction (LLE) strategies are commonly used for industrial separation and purification in hydrometallurgy as they provide acceptable enrichment needed for many extraction applications. However, separation and purification of REEs by such technique requires the treatment of a large volume of solvents over continuous, repeated steps, which lead to significant amounts of undesired and radioactive wastes. In comparison, liquid-solid extraction is a simpler and greener alternative. Chromatographic-based resins (ion-exchange, IEC, or extraction resins, EXC) have been used with respect to REEs separation and purification. As early as 1947, Spedding [7] has demonstrated that ammonium citrate / citric acid could selectively elute REEs loaded onto a Amberlite IR-100 (strong cationic ion-exchanger). Similarly to extraction performed by LLE, shifting stability of coordinated REEs, owing to change in ionic radius resulting from the lanthanide contraction, enables elemental separation. Other studies using anion-exchange resins where REEs are complexed with negatively charged ligands have also been reported.[8] More recently, liquid-liquid extraction on a solid support (also referred as EXC) has been applied to the separation and purification of REEs.[9] In most EXC resins, a selective ligand is dissolved in an hydrophobic organic phase which is impregnated on a solid support. Among the selective ligands reported, diglycolylamide (DGA) derivatives have demonstrated interesting extractive properties for REEs. Recently, researchers attempted to replace the organic phase, in which the extractant was dissolved, by an ionic liquid which was entrapped into a silica sol–gel composite for the extraction of La(III). Unfortunately, the impregnation strategies employed resulted in EXC materials that demonstrated pronounced leaching of the stationary liquid phase which translated into cross-contamination and lack of reusability,[10–13] thus hampering their applicability. To overcome such issues, it has been proposed to chemically anchor the extracting agent to the solid support. To do so, Zhang suggested first a polymeric

Dr. J. Florek, F. Chalifour, Prof. D. Larivière, Prof. F. Kleitz
Department of Chemistry
Centre de Recherche sur les Matériaux Avancés (CERMA) and Centre en Catalyse et Chimie Verte (C3V)
Université Laval
Quebec, G1V 0A6, QC, Canada
E-mail: dominic.lariviere@chm.ulaval.ca; freddy.kleitz@chm.ulaval.ca
F. Bilodeau
Hydro-Quebec Production
Gentilly-2 Nuclear Power Plant
Gentilly, G9H 3X3, QC, Canada

DOI: 10.1002/adfm.201303602

composite which included a DGA-derivative simply deposited (i.e., adsorbed) on a macroporous silica support (particle size between 40–60 µm, pores ≈ 600 nm).[14] The choice of macroporous silica was motivated by the fact that such a support could exhibit rapid sorption and elution kinetics, high mechanical strength and a reduced pressure loss in a packed column.

With the recent development of the area of ordered mesoporous materials, where silica structures with high surface area (≈1000 m^2 g^{-1}), high pore volume (>1 cm^3 g^{-1}) and well-defined pore size in the nanometer range can easily be prepared in aqueous conditions by cooperative self-assembly, of inorganic precursors and amphiphilic structure-directing agents,[15] it is legitimate to wonder if such nanoporous supports could provide enhanced separation and analytical performances.

These porous materials exhibit abundance of silanol groups on the mesopore surfaces, allowing for adequate functionalization through chemical grafting,[16] which would eliminate the leaching and cross-contamination observed in EXC. In addition, morphology and dimension of the particles can also be controlled.[17] Furthermore, tailoring of pore size, pore shape and pore connectivity of these materials is possible in order to optimize adsorption and diffusion parameters, critical in liquid-solid separation processes. Such mesoporous materials were proven promising for chromatography applications in selective capture and removal of heavy metals and/or radioisotopes.[18] In contrast to the previously reported macroporous system investigated for REEs separation,[14] mesoporous materials exhibit exceedingly higher surface area allowing for a substantially enhanced adsorption capacity and high contact efficiency. Moreover, such highly porous architectures may solve the problem associated to increasing backpressure of chromatographic-based resins, as in the case of well packed chromatographic columns with small particles sizes. It is known that, resolution of high-performance chromatographic-based resins is also related to the type of rigid support.[19]

Following our previous success with actinide adsorption,[20] we herein propose to use diglycolylamide (DGA)-modified mesoporous KIT-6 silica[21] as a potential candidate for the REEs separation. In our strategy, the DGA ligand is chemically grafted to the silica surface, which enables the resulting hybrid materials to be cycled and regenerated, a key feature in the development of sustainable and cost-effective resin-type materials minimizing waste production. The choice of the KIT-6 silica is motivated by the highly interconnected nature of the pore network of this material, which is expected to reduce risks of pore blocking and be beneficial for diffusion of liquids through the system.[20] Extraction of REEs was performed in a solid-liquid system, and distribution coefficients (K_d)[22] from batch extraction tests were estimated. These new sorbents are stable upon recycling and show greater selectivity than commercially available DGA-resins under the extraction conditions tested. Most importantly, we reveal a much higher affinity of our sorbents for the separation of heavier lanthanides (i.e., yttric earths), being most relevant for the electronic industries.

2. Results and Discussion

2.1. Materials

The synthesis approach for the modified KIT-6 materials is depicted in **Scheme 1** and details of the experimental protocol are found in the Experimental Section. Post-synthesis functionalization of KIT-6 silica with the appropriate ligand was performed according to a standard procedure in dry toluene under reflux and N_2 atmosphere.[16] Surface modification was performed, either in one-step, or two-step (step-by-step) sequence, yielding samples designated as KIT-6-N-DGA-1 and KIT-6-N-DGA-2, respectively.

2.1.1. Structural Characterization and Porosity Assessment

First, the mesoscopic 3-D pore organization of the functionalized KIT-6 materials was verified by transmission electron

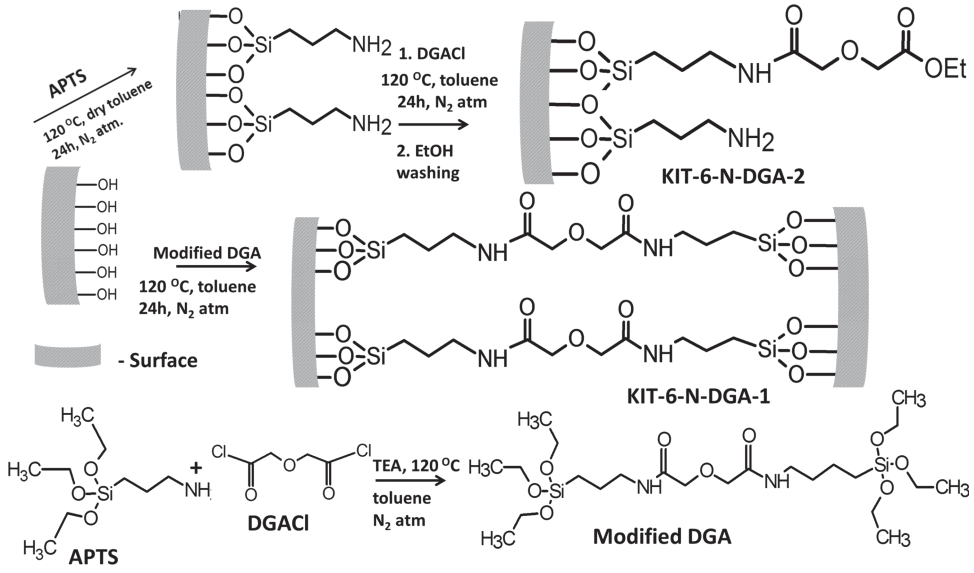

Scheme 1. One-step and two-step modifications of the surface of KIT-6 silica to generate the mesoporous rare-earth element (REE) sorbents.

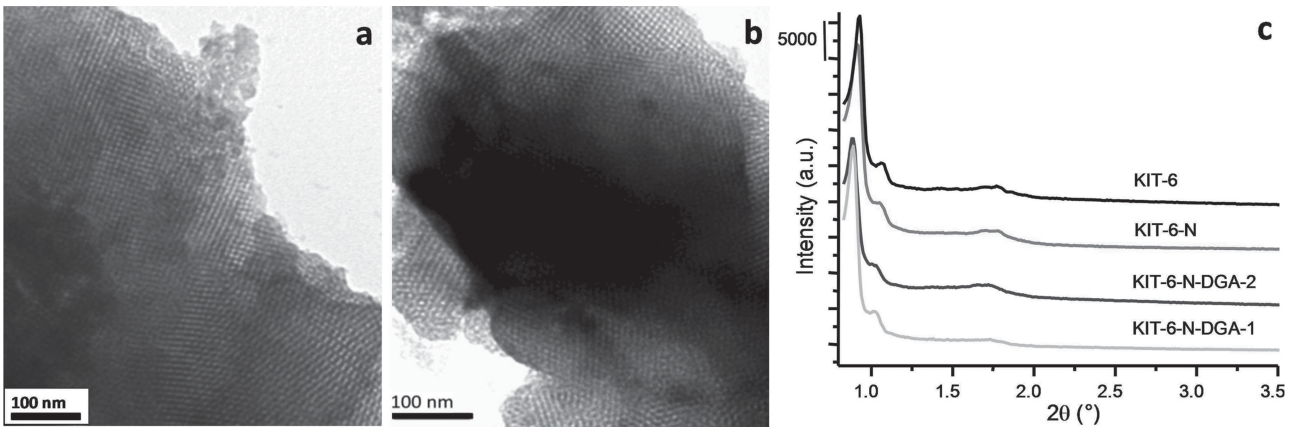

Figure 1. Representative TEM images for the a) KIT-6-N-DGA-1, b) KIT-6-N-DGA-2 sorbents, and c) low-angle powder XRD patterns of pristine and modified materials.

microscopy (TEM), high-resolution scanning electron microscopy (HR-SEM), and low-angle powder X-ray diffraction (XRD), as illustrated in **Figures 1**, **2**. In all cases, the pore mesostructure is shown to be commensurate with the *Ia*3*d* symmetry,[20,21] as expected for KIT-6 derived materials. High-resolution SEM images of the functionalized hybrids (see

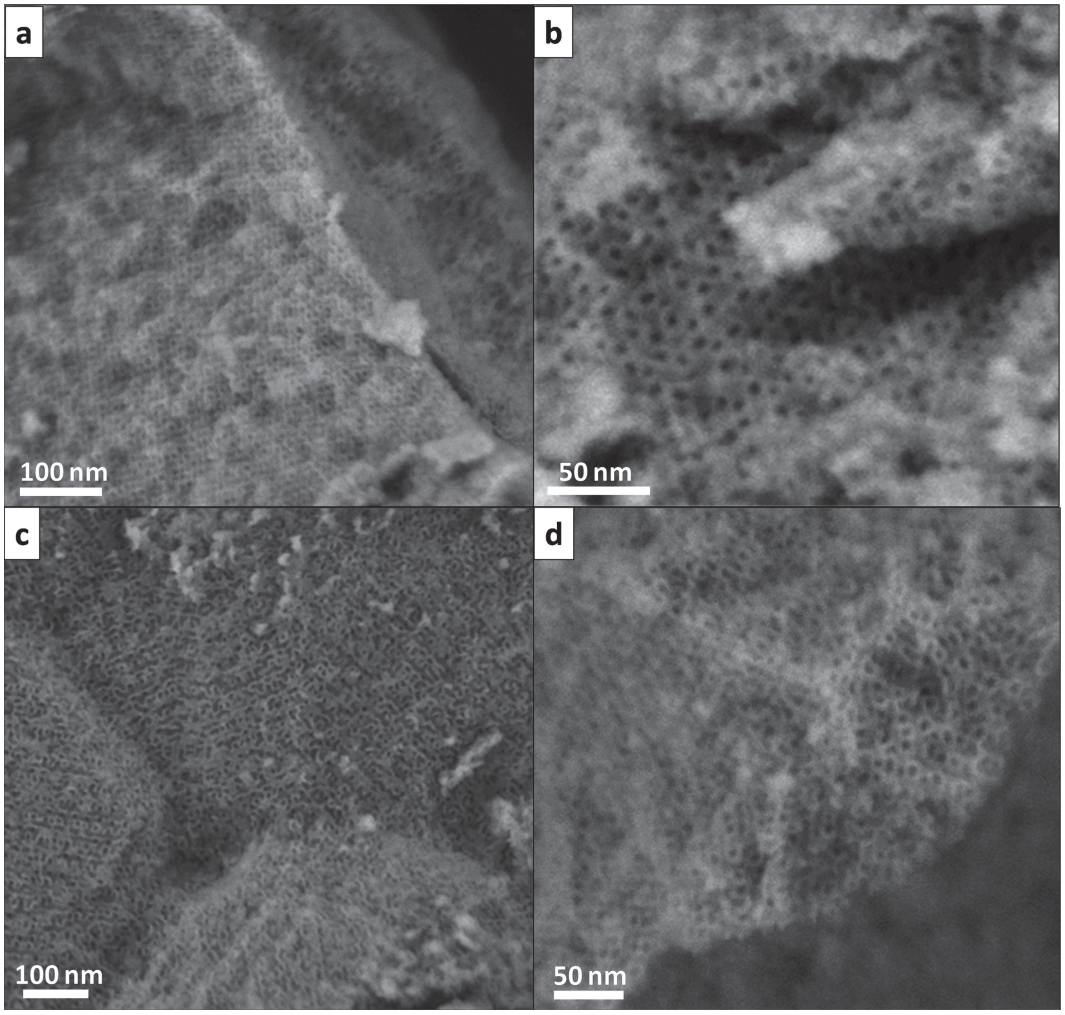

Figure 2. High-resolution SEM images (overviews and magnified areas) of the a,b) organic-inorganic hybrid KIT-6-N-DGA-1 and c,d) KIT-6-N-DGA-2 sorbents.

Table 1. Physicochemical parameters obtained by N_2 physisorption measurements (–196 °C) for the different samples.

Sample	S_{BET} [m^2 g^{-1}]	V_{pore} [cm^3 g^{-1}]	Pore size [nm]
KIT-6	831	1.17	8.4
KIT-6-N	392	0.68	7.8
KIT-6-N-DGA-2	351	0.57	7.0
KIT-6-N-DGA-1	621	0.81	7.6

Figure 2) confirm that, although the materials have been subjected to several grafting-Soxhlet sequences (see Experimental section), the ordered pore structure remains intact and, obviously, fully accessible from the outside surface of the particles, similarly to the parent pure silica.[21d]

The physicochemical parameters derived from the N_2 sorption analysis are compiled in **Table 1** and the corresponding values for the specific surface area (BET), pore volume and pore size distribution (PSD) for the pristine and functionalized materials are shown in Figure S1 (SI; Supporting Information). All of the modified materials exhibit typical type IV isotherms with a well-pronounced capillary condensation step and distinctive H1 hysteresis loop, characteristic of large cylindrical mesopores.[21b] After anchoring of the organic ligand (DGA) on the silica support, the shape of the hysteresis loop is well maintained, but the capillary condensation step is obviously shifted to the lower values of relative pressure (P/P_o), indicative of a decrease in the pore size upon surface modification. This decrease in pore size is more pronounced for the material modified by the two-step (step-by-step) procedure (KIT-6-N-DGA-2), that is, from 8.1 to 7.0 nm compared to the one-step procedure (KIT-6-N-DGA-1), that is, from 8.1 to 7.6 nm. Similar evolution is observed for the surface area and pore volume; with KIT-6-N-DGA-2 exhibiting the lowest values (Table 1).

2.1.2. Surface Characterization

To confirm the covalent attachment of the organic species on the KIT-6 surface, solid state NMR, IR and thermogravimetric analyses were performed. Considering first the two-step procedure, the ^{13}C CP (MAS) NMR spectrum of KIT-6 which is first modified with amine groups, that is, KIT-6-N, showed presence of three peaks assigned to the methylene carbons in the aminopropyl group[23] linked to the silica surface (**Figure 3**). The successful modification of KIT-6 silica with the DGA molecule was then validated by the presence of two additional bands in the ^{13}C CP/NMR spectra of the KIT-6-N-DGA-2 sample, in comparison to KIT-6-N. These two bands appear at ≈ 68 and 170 ppm, and are characteristic of the CH_2 group linking the carbonyl group and ether oxygen;[24] the former band is assigned to the amide bond in the DGA molecule.[25] An additional peak at 60 ppm assigned to remaining ethoxy groups in (-Si-O-CH_2-CH_3)[26] is also clearly visible. In case of the one-step modification (KIT-6-N-DGA-1), similar features are observed and the spectrum resembles that of KIT-6-N-DGA-2. Note that, the peak at 60 ppm is somewhat less pronounced for KIT-6-N-DGA-1. In the case of KIT-6-N-DGA-2, unreacted chlorine groups of diglycolyl chloride (DGACl) may be substituted by ethoxy species upon washing with ethanol via esterification (Scheme 1), and correspondingly, the ^{13}C NMR signal at 60 ppm could be more pronounced compared to KIT-6-N-DGA-1. In both cases, the absence of a band at ≈180 ppm (indicative of the presence of COOH or COCl groups)[27] is in line with the structures proposed in Scheme 1 (DGA grafted by the two sides in KIT-6-N-DGA-1). The two additional small bands that are visible on the ^{13}C NMR spectra of the DGA-modified materials are spinning side-bands (see Figure 3a). Covalent attachment of the DGA molecule was further confirmed by ^{29}Si MAS NMR, which reveals in both cases signals originating from Tn groups associated to the silicon of the covalently grafted silane (Figure 3b). The peaks at –66, –58, and –48 ppm are assigned

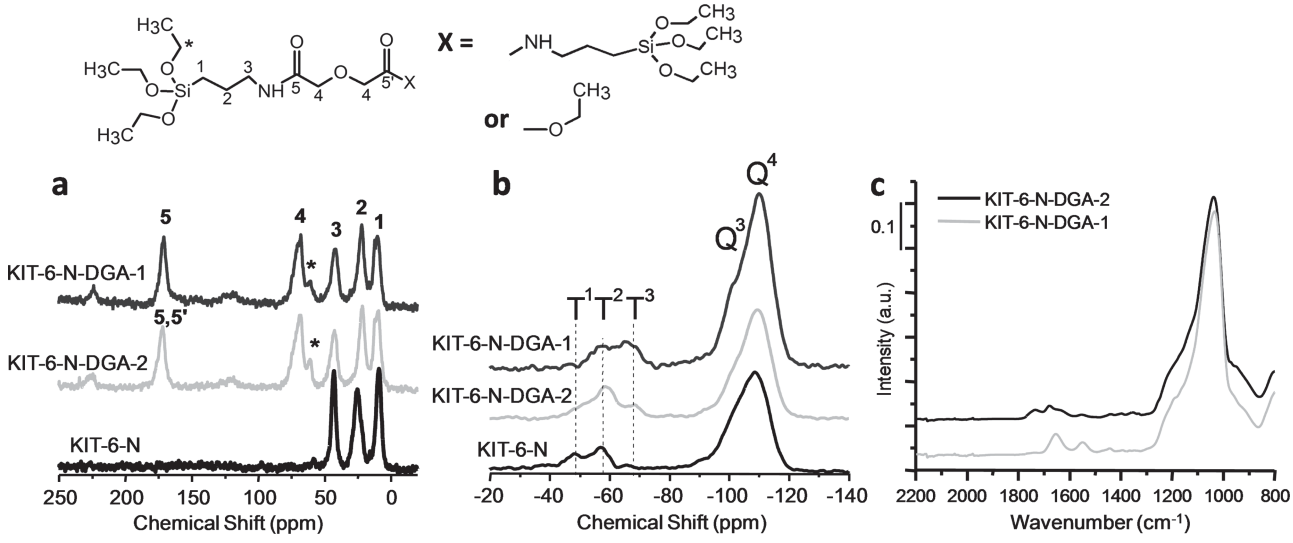

Figure 3. Solid state a) ^{13}C CP/NMR, b) ^{29}Si MAS NMR, and c) IR spectra for the different functionalized mesoporous materials. The two additional small bands visible on the ^{13}C NMR spectra of KIT-6-N-DGA-1 and -2 are spinning side-bands of the carbonyl peak (**5, 5′**).

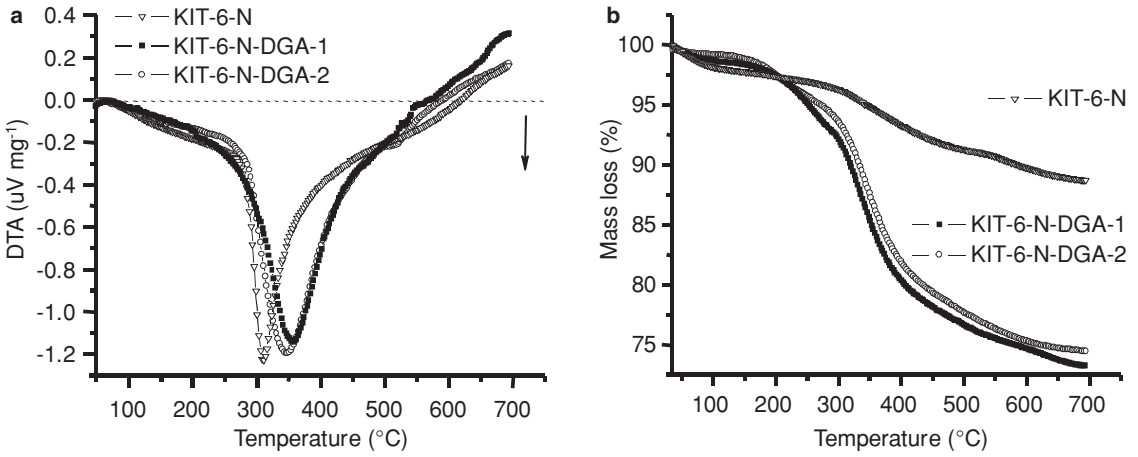

Figure 4. a) The differential thermal analysis (DTA) and b) thermogravimetric analysis curves of the DGA-modified KIT-6 silica samples (as indicated). The arrow in the DTA graph indicates direction of exothermic process.

to T^3 ($(SiO)_3Si$-R), T^2 ($(SiO)_2(OR)Si$-R) and T^1 ($(SiO)(OR)_2Si$-R) species, respectively.[28]

Nevertheless, KIT-6-N-DGA-1 possesses almost equal ratio of T^3 and T^2 species, while the material modified by the step-by-step procedure showed dominance of T^2 groups. It is thus evident that the two different modification procedures lead to distinct anchoring environments for the grafted DGA species on the silica surface (Scheme 1). The presence of the amide bond in the modified hybrid solids was also confirmed by the bands visible at 1657 and 1550 cm^{-1} in the FTIR spectra, which are characteristic for Amide I (CO stretching) and Amide II band (NH deformation, CN stretching), respectively (Figure 3c).[29] In addition, KIT-6-N-DGA-2 also showed the presence of a second carbonyl band (CO stretching), which is in agreement with the different DGA structures of the grafted species as suggested in Scheme 1.

Thermogravimetric analysis (TGA) of both DGA-modified materials indicates a total weight loss at about 24% (**Figure 4**). The thermal decomposition of the functionalized sorbents occurred in the interval of temperatures between 150 and 650 °C. A broad exothermic effect attributed to the decomposition of DGA was observed between 340 and 360 °C. A slight shift to lower temperatures (345 °C) was observed for KIT-6-N-DGA-2, compared to the one-step KIT-6-N-DGA-1 sample (356 °C), which might be correlated to residual "free" $-NH_2$ groups on the surface of KIT-6-N-DGA-2 (in agreement with the lower temperature peak at 310 °C observed for KIT-6-N). The amounts of carbon, nitrogen and hydrogen for all modified samples were obtained by CHN elemental analysis and the respective values are given in Table S1 (SI). For both DGA-functionalized samples, the contents in these elements are similar. Moreover, the Mohr's method was used to determine chlorine concentration in both KIT-6-N-DGA samples, and the calculated values are given in Table S1 (SI). The lack of residual chloride ions in both samples further corroborates a complete substitution of the chlorine atoms in the diglycolyl chloride molecule (DGACl).

X-ray photoelectron spectroscopy (XPS) analyses which were performed on the functionalized materials also confirmed the presence of the DGA organic moieties on the surface of the KIT-6-N-DGA materials (Figure S2, SI). Furthermore, we observed that the intensities of the peaks related to the amide bond[30,31] visible in the DGA-modified materials are higher and better resolved for the sample modified through the one-step procedure, i.e., KIT-6-DGA-1, compared to the two-step procedure, that is, KIT-6-N-DGA-2. These XPS data are in agreement with the above results from IR, NMR, and TGA.

2.2. Extraction Studies

Extraction of REEs using the modified KIT-6 materials was evaluated in terms of the K_d values (K_d – distribution coefficients; mL g^{-1}) and compared with a commercially available DGA resin (**Figure 5** and SI, Figure S3). K_d were calculated by the following Equation 1:[22b,32,33]

$$K_d = \frac{C_i - C_f}{C_f} \times \frac{V}{m} \quad (1)$$

Where, C_i and C_f are initial and final concentration, respectively; and V and m are volume of solution and mass of sorbent taken for the batch extraction tests, respectively.

As documented in the literature, the higher the K_d value, the better is the extraction capacity.[33] Using the materials developed in the experimental setup a K_d of 500 would represent a retention of about 50% whereas a value of 5000 would translate in over 90% of the analyte retained on the resin. Results from the batch extraction tests, with a mixture of lanthanides, are shown in Figure 5a as a function of K_d value versus the atomic number. The respective standard deviations are provided for these values of distribution coefficient (K_d) in Figure S3 (SI). From our results, it is obvious that the modification of KIT-6 with DGA enhances substantially the K_d value for lanthanides, as compared to the pure silica (KIT-6) or the amino-modified precursor (KIT-6-N). Selectivity of Eichrom DGA resins for the different lanthanides has been documented.[22] However, in comparison to such a resin, the uptake of REEs is significantly

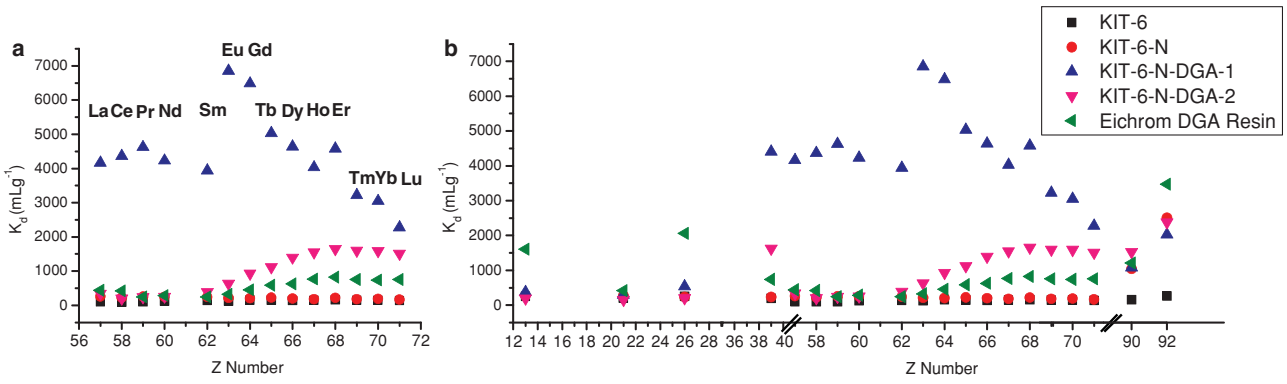

Figure 5. Distribution coefficients (K_d) values for the functionalized hybrid materials and the commercial DGA-resin, as a function of the atomic number *Z*: a) K_d for a mixture of all the lanthanides; b) Competitive K_d values for REEs in the presence of aluminum, iron, thorium and uranium in the extraction mixture. For the standard deviations (error bars) of the analyses, see the corresponding extended Figure S3 in SI.

improved using the KIT-6-N-DGA materials, and their K_d values are several times higher than those of the commercial counterpart.[33]

Most importantly, the KIT-6-N-DGA samples clearly express different selectivity toward lanthanides as a function of atomic radiuses, being much higher than that of the commercial resin (see Figures 5 and SI, Figure S3). A change in selectivity is clearly more pronounced for the one-step KIT-6-N-DGA-1 material. In contrast to the commercial DGA resin, the maximum selectivity for the KIT-6-N-DGA-1 sorbent is shifted to REEs with slightly lower atomic numbers, and the maximum K_d value (K_d = 6856 mL g^{-1}) is obtained for Eu (Z = 63). In comparison, standard DGA-based resins showed a maximum K_d value for Er in the conditions tested, but otherwise exhibit maximum K_d value for Tm and Lu (in 0.5 M and 0.05 M HNO_3, respectively) in the case of TODGA (N,N,N′,N′-tetra-n-octyldiglycolamide; Normal DGA Resin) or for Ho (1 M HNO_3) using the TEHDGA (N,N,N′,N′-tetrakis-2-ethylhexyldiglycolamide; Branched DGA Resin).[22]

Comparing the uptake of lanthanides between the different DGA-modified KIT-6, the much higher K_d values and selectivity (K_d for elements with atomic number in the range 57-64) observed for KIT-6-N-DGA-1 might suggest a more uniform dispersion the DGA molecules, in comparison to the two-step material, and/or more favorable ligand structure (see Scheme 1). In addition, differences between these two materials can also originate from the presence of residual -NH_2 groups on the surface of KIT-6-N-DGA-2, which are absent in KIT-6-N-DGA-1. Primary amines are known to be excellent Lewis base for coordinating REEs, however with no size specificity (as otherwise provided by chelation of DGA) leading to poorer selectivity. Nevertheless, the distinct selectivities obtained for the two sorbents suggest that it is possible to further fine tune the ligand environment on the surface in order to target each lanthanide with high specificity. Further studies are needed to achieve a single-REE-selective ligand design with optimized surface environment.

K_d values for all REEs in the presence of trivalent competing ions of environmental and mining relevance, that is, Al^{3+}, Fe^{3+}, are presented in Figure 5b. For both KIT-6-N-DGA samples, significantly higher extraction capacities were observed towards REEs, indicating a low degree of competition to the chelating sites for these cations. Surprisingly, the extraction capacities for Al^{3+} and Fe^{3+} using the impregnated (commercial) DGA resin were higher than for REEs, which highlights a crucial role of the silica support with anchored DGA in the extraction process. Moreover, decontamination of REEs from radioactive side products, such as U and Th, is one of the key issues and challenge in REEs extraction. According to our results in Figure 5b, separation factors (SF) that allow for the efficient and commercially profitable separation of Th and U from REEs[34] were obtain only for the one-step KIT-6-N-DGA-1 material, with Eu/Th = 6.3 and Eu/U = 3.4, respectively.

At present, one may speculate that the selective extraction trend observed for the KIT-6-N-DGA materials is due to a combination of steric effects and electrostatic interactions that may be more pronounced in the presence of the solid support than in liquid phase. The present results establish that the rigid structure of the KIT-6 material could provide a favorable geometry of the organic functionalities for complexing trivalent metal ions through two carbonyl oxygen atoms and the ether oxygen, thus forming more stable chelate rings.[35] Further, it is reasonable to assume that the silica skeleton limits the degree of liberty of the ligands which are immobilized on the surface, favoring chelation of ions of a certain radius range only (i.e., 85–97 pm).

2.2.1. Reusability Test

Commercial extraction resins are plagued with issues such as their lack of reusability and the elution of organic extractant/stationary phase. In comparison, grafting DGA on KIT-6 silica affords much more robust materials. Cycling tests for the REEs extraction were performed in the case of KIT-6-N-DGA-1, to probe the regeneration ability of our systems. From **Figure 6**, it is evident that the KIT-6-N-DGA sorbents can be reused, indicative of the excellent stability of the organic ligands on the silica surface. The stability of the organic moieties after extraction was also confirmed by TGA and solid state NMR (Figure S4, SI). No significant changes in both the amount and the integrity

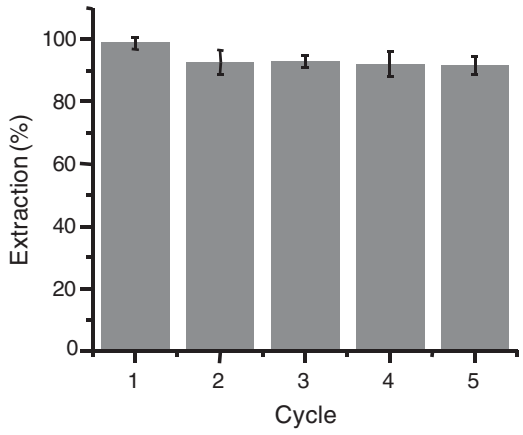

Figure 6. Reusability tests for the KIT-6-N-DGA-1 sorbent (batch extraction is performed using a mixture of all the lanthanides).

of the organic groups in the used material could be seen after REEs extraction.

3. Conclusions

In summary, we have reported the first examples of mesoporous diglycolamide-modified KIT-6 hybrid materials, obtained by a controlled ligand grafting on the silica support (KIT-6), to be used for extraction/separation of lanthanides. One-step and two-steps grafting procedures could generate materials exhibiting distinct bonding capacities, which could be related to favorable geometries achieved during synthesis. In particular, the sample prepared through the one-step method, that is, KIT-6-N-DGA-1, clearly showed much higher extraction performances than commercial resins. It also exhibited specificity towards Eu and Gd and low competitive behavior with other non-lanthanide trivalent ions and actinides, which are problematic for the commercial extraction of REEs. Efficient reusability of the materials was also demonstrated. One objective with this new system will be to minimize as much as possible the number of extraction steps used for the purification of REEs. Functionalized nanoporous materials possessing high surface area and high pore volume can offer high contact efficiency with solutions and high adsorption capacities, while preserving adequate flow and transport properties, if properly structured. Using such materials may indeed enable us to reduce substantially the number of steps needed for separation of these critical elements, and thus decrease both the required time and waste production.

4. Experimental Section

Synthesis of Ordered Mesoporous KIT-6 Silica: High quality KIT-6 silica was obtained following the procedure reported by Kleitz et al.[21a] Briefly, 9.0 g of Pluronic P123 ($EO_{20}PO_{70}EO_{20}$, Sigma-Aldrich) was dissolved in 325 g of distilled water and 17.40 g HCl (37%) was added under vigorous stirring. After complete dissolution, 9.0 g of n-butanol (BuOH, Aldrich, 99%) was added. The mixture was left under stirring at 35 °C for 1 h, after which 19.35 g of tetraethoxysilane (TEOS, Acros, 99%) was added at once to the homogenous clear solution. The molar composition of the starting reaction mixture was TEOS/P123/HCl/H_2O/BuOH = 1.0/0.017/1.83/195/1.31. This mixture was left under stirring at 35 °C for 24 h, followed by an aging step at 100 °C for 48 h under static conditions. The resulting solid product was then filtered and dried for 48h at 100 °C. For template removal, the as-synthesized silica powder was first shortly slurried in ethanol-HCl mixture and the resulting material was subsequently calcined at 550 °C for 2 h.

One-Step Modification Procedure (KIT-6-N-DGA-1): For the one-step modification of KIT-6, first a DGA derivative of the aminosilane was prepared. The synthesis is briefed as follows: 2 mL (8.5 mmol) of (3-aminopropyl)triethoxysilane (APTS, Sigma-Aldrich, 98%) was added to 20 mL of dry toluene under inert atmosphere (N_2) and reflux conditions. After that, 0.46 mL (3.8 mmol) of diglycolyl chloride (DGACl, Sigma-Aldrich, 95%) was dissolved in 30 mL of dry toluene and added at once to the solution of APTS. Triethylamine (TEA, Alfa Aesar, 99%) was added as a catalyst (1.2 mL). The resulting mixture was left under stirring for 24 h under reflux conditions and N_2 flow. This mixture of the modified silane was then used without further purification. Note that, the structure of the modified silane was confirmed by liquid ^{1}H NMR (see SI).

For the surface modification of KIT-6 silica, 1 g of activated KIT-6 material (treated overnight at 150 °C under vacuum) was dispersed in 50 mL of dry toluene, under inert atmosphere (N_2 flow). Then, a catalytic amount of triethylamine (TEA, Alfa Aesar, 99%) was added to the suspension of KIT-6 silica, and the above solution of the DGA-modified silane was added at once to this suspension, under inert atmosphere. The resulting mixture was left under stirring for 24h under reflux conditions. After cooling to room temperature, the suspended solid product was filtered, washed thoroughly with toluene and ethanol three times, and then dried at 70 °C overnight in air. Un-reacted silane molecules were removed by Soxhlet extraction in dichloromethane for 6 h. The resulting product was noted as KIT-6-N-DGA-1.

Two-Steps (Step-by-Step) Functionalization (KIT-6-N, KIT-6-N-DGA-2): For the surface modification of KIT-6, 1 g of activated KIT-6 material (treated overnight at 150 °C under vacuum) was dispersed in 75 mL of dry toluene, in inert atmosphere (N_2 flow). Then, 2 mL of (3-aminopropyl) triethoxysilane (APTS, Sigma-Aldrich, 98%) was added at once to the dispersion. The resulting mixture was left under stirring for 24 h under reflux conditions. After cooling to room temperature, the suspended solid product was filtered, washed thoroughly with toluene and ethanol three times, and then dried at 70 °C overnight in air. Unreacted aminosilane molecules were removed by Soxhlet extraction in dichloromethane for 6 h. The resulting material was designated as KIT-6-N and used for the subsequent functionalization step, in which diglycolyl chloride (DGACl, Sigma-Aldrich, 95%) was introduced. For this modification step, 0.5 g of the activated KIT-6-N material (treated overnight at 70 °C under vacuum) was dispersed in 50 mL of dry toluene, under inert atmosphere (N_2 flow). Then, diglycolyl chloride (DGACl, Sigma-Aldrich, 95%) was dissolved in 10 mL dry toluene and added at once to this dispersion. The resulting mixture was left stirring for 24 h under reflux conditions. After cooling to room temperature, the suspended solid product was filtered, washed thoroughly with toluene and ethanol three times, and then dried at 70 °C overnight in air. Unreacted diglycolyl chloride molecules were removed by Soxhlet extraction in dichloromethane for 6 h. The resulting product was noted as KIT-6-N-DGA-2.

Materials Characterization: N_2 adsorption-desorption isotherms were measured at –196 °C (77 K) using an Autosorb-1-MP sorption analyzer (Quantachrome Instruments, Boyton Beach, Fl, USA). Prior to the analysis, the samples were outgassed for 12h at 200 °C (parent silica) or at 80 °C for 8 h (functionalized sorbents), under turbomolecular pump vacuum. These degassing conditions were chosen in order to preserve the integrity of the organic moieties in the organosilica materials, as implemented previously.[20,36] The specific surface area (S_{BET}) was determined using the Brunauer-Emmett-Teller equation in the range $0.05 \leq P/P_0 \leq 0.20$, and the total pore volume (V_{pore}) was measured at $P/P_0 = 0.95$. Pore size distributions were calculated from the desorption branch using nonlocal density functional theory (NLDFT) methods

considering sorption of nitrogen at –196 °C in cylindrical silica pores.[21c] Thermogravimetric analysis-differential thermal analysis (TG-DTA) was performed using a Netzsch STA 449C thermogravimetric analyzer, under the air flow of 20 mL min^{-1} with a heating rate of 10 °C min^{-1}. Solid state MAS NMR spectra were obtained on a Bruker DRX300 MHz spectrometer. The ^{29}Si MAS NMR spectra were measured at 59.60 MHz using 7 mm rotors spinning at 4 kHz. The 75.4 MHz ^{13}C CP-MAS spectra were recordered using a 7 mm rotor spinning at 4 kHz. The chemical shifts are reported in ppm relative to tetramethylsilane (TMS) for ^{29}Si and relative to adamantane for ^{13}C. FTIR spectra were recorded using a Nicolet Magna FTIR spectrometer with a narrow band MCT detector (Specac Ltd., London). Spectra were obtained from 128 scans with a 4 cm^{-1} resolution. Transmission electron microscopy (TEM) was performed using a JEOL JEM 1230 at an accelerating voltage of 80 kV with a LaB_6 filament. For the specimen preparation, the powders were dispersed in methanol and sonicated during 15 min in a sonic bath. Then, 5 µL of the suspension were placed onto a nickel/Formvar grid and allowed to dry before measurements. Scanning electron microscopy (SEM) images were obtained with a FEI Magellan 400 at a low landing energy (1.0 kV), without metal coating (KAIST, Daejeon, Republic of Korea). X-ray photoelectron spectroscopy (XPS) measurements were conducted on a Kratos AXIS-ULTRA spectrometer with a monochromatic Al X-ray source operated at 300 W. Survey scans were recorded with a passing energy of 160 eV and incremental steps of 1 eV. Low-angle powder X-ray diffraction (XRD) patterns were recorded on a Rigaku Multiplex instrument operated at 2 kW, using Cu Kα radiation (KAIST, Daejeon, Republic of Korea). The XRD scanning was performed under ambient conditions in steps of 0.01, with an accumulation time of 0.5 s. Elemental analysis was performed by the combustion method using a CHNS Analyzer Flash 2000, Thermo Scientific.

Extraction Experiments and Reusability Tests: Batch extraction tests: Solutions of REEs (Sc, Y, La, Ce, Pr, Nd, Sm, Eu, Gd, Tb, Dy, Ho, Er, Tm, Yb, Lu) and additional ions, that is, Al, Fe, Th, and U in HNO_3 (pH = 4) were prepared from the standards solutions (Plasma, Cal, SCP Science), in order to obtain the final concentration of extraction solution of 2 µg L^{-1} for each element tested. A solution of 2 µg L^{-1} of Tl was chosen as the internal standard. The commercial DGA resin was purchased from Eichrom (N,N,N′,N′-tetra-n-octyldiglycolamide Resin; DGA Resin-Normal; USA Lisle, IL). The solution/solid ratio was fixed to 500 (V/m). The samples (10 mg) were stirred in an orbital shaker for 30 min and subsequently the supernatant was filtered through a 0.2 µm syringe filter. All experiments were done three times and the average values are given. The initial and final concentrations of the REEs in solutions were determined by ICP-MS (ICP-MS-8800, Agilent Technologies, Triple Quad) measurements.

Sorbent Reusability Studies: after 30 min of extraction test, the extraction solution of REEs was separated from the KIT-6-N-DGA-1 material (30 mg) by centrifugation (the solution/solid ratio (V/m) during the extraction procedure was fixed to 500). The un-retained REEs fraction was collected and analyzed by ICP-MS. Subsequently, the sorbent was rinsed with 10 mL of 0.1 M $(NH_4)_2C_2O_4$ and 10 mL of high purity water. The material was then reconditioned using 4% HNO_3 and was used in subsequent extraction tests by repeating the procedure above-mentioned to achieve 5 extraction-elution cycles.

Supporting Information

Supporting Information is available from the Wiley Online Library or from the author.

Acknowledgements

This work was supported by the Natural Sciences and Research Council of Canada through a Strategic Project Grant. The authors thank Dr. Y. Seo and Prof. R. Ryoo (KAIST, Daejeon, Republic of Korea) for providing the low-angle powder XRD data and high resolution SEM images of the samples.

Received: October 22, 2013
Revised: November 16, 2013
Published online: January 16, 2014

[1] a) J. F. Tremblay, *Chem. Eng. News* **2012**, *90*, 14; b) S. Massari, M. Ruberti, *Resources Policy* **2012**, *38*, 36.
[2] P. Maestro, D. Huguenin, *J. Alloys Compd.* **1995**, *225*, 520.
[3] D. J. Hanson, *Chem. Eng. News* **2011**, *89* , 28.
[4] C. K. Gupta, N. Krishnamurthy, *Int. Mater. Rev.* **1992**, *37*, 197.
[5] L. V. Tsakanika, M. Th. Ochsenkuhn-Petropoulou, L. N. Mendrinos, *Anal. Bioanal. Chem.* **2004**, *379*, 796.
[6] T. Uda, K. T. Jacob, M. Hirasawa, *Science* **2000**, *289*, 2326.
[7] F. H. Spedding, *J. Am. Chem. Soc.* **1947**, *69*, 2812.
[8] a) H. Hamaguchi, A. Ohuchi, N. Inuma, R. Kuroda, *J. Chromatogr.* **1964**, *16*, 396; b) R. G. Fernandez, J. I. Garcia Alonso, *J. Chromatogr. A* **2008**, *1180*, 59.
[9] a) B. R. Reddy, S. Radhika, B. N. Kumar, *Chem. Eng. J.* **2010**, 160; b) S. K. Menon, H. Kaur, S. R. Dave, *React. Funct. Polym.* **2010**, *7*, 692; c) Q. Jia, Z. H. Wang, D. Q. Li, C. J. Niu, *J. Alloys Compd.* **2004**, *374*, 434; d) B. Kronholm, C. Anderson, P. R. Taylor, *JOM* **2013**, *65*, 1321.
[10] D. Larivière, T. A. Cumming, S. Kiser, C. Li, R. Cornett, *J. Anal. At. Spectrom.* **2008**, *23*, 352.
[11] C.-S. Kim, C.-K. Kim, K. J. Lee, *J. Anal. Chem.* **2002**, *74*, 3824.
[12] a) E. P. Horwitz, R. Chiarizia, M. L. Dietz, H. Diamond, D. M. Nelson, *Anal. Chim. Acta.* **1993**, *281*, 361; b) E. P. Horwitz, M. L. Dietz, R. Chiarizia, H. Diamond, *Anal. Chim. Acta.* **1992**, *266*, 25.
[13] V. N. Epov, K. Benkhedda, R. J. Cornett, R. D. Evans, *J. Anal. At. Spectrom.* **2005**, *20*, 424.
[14] A. Zhang, C. Mei, Y. Wei, M. Kumagai, *Adsorpt. Sci.Techn.* **2007**, *25*, 257.
[15] a) C. T. Kresge, M. E. Leonowicz, W. J. Roth, J. C. Vartuli, J. S. Beck, *Nature* **1992**, *359*, 710; b) D. Zhao, Y. Wan, *Chem. Rev.* **2007**, *107*, 2821.
[16] F. Hoffmann, M. Cornelius, J. Morell, M. Froba, *Angew. Chem. Int. Ed.* **2006**, *45*, 3216.
[17] G. J. A. A. Soler-Illia, C. Sanchez, B. Lebeau, J. Patarin, *Chem. Rev.* **2002**, *102*, 4093.
[18] a) T. Sangvanich, V. Sukwarotwat, R. J. Wiacek, R. M. Grudzien, G. E. Fryxell, R. S. Addleman, C. Timchalk, W. Yantasse, *J. Hazard Mater.* **2010**, *182*, 225; b) I. Sierra, D. Pérez-Quintanilla, *Chem. Soc. Rev.* **2013**, *42*, 3792; c) P. Wang, I. M. C. Lo, *Water. Res.* **2009**, *43*, 15, 3727; d) N. Calin, A. Galarneau, T. Cacciaguerra, R. Denoyel, F. Fajula, *C.R. Chim.* **2010**, *13*, 199; e) A. Walcarius, L. Mercier, *J. Mater. Chem.* **2010**, *20*, 4478; f) Z. Wu, D. Y. Zhao, *Chem. Commun.* **2011**, *47*, 3332.
[19] a) D. T. Nguyen, D. Guillarme, S. Rudaz, J.-L. Veuthey, *J. Sep. Sci.* **2006**, *29*, 1839; b) U. D. Neue, HPLC Columns: Theory, Technology, and Practice, 1st ed., Wiley-VCH, NY **1997**.
[20] a) P. J. Lebed, K. de Souza, F. Bilodeau, D. Larivière, F. Kleitz, *Chem. Commun.* **2011**, *47*, 11525; b) P. J. Lebed, J.-D. Savoie, J. Florek, F. Bilodeau, D. Larivière, F. Kleitz, *Chem. Mater.* **2012**, *24*, 4166.
[21] a) F. Kleitz, S. H. Choi, R. Ryoo, *Chem. Commun.* **2003**, 2136; b) T.-W. Kim, F. Kleitz, B. Paul, R. Ryoo, *J. Am. Chem. Soc.* **2005**, *127*, 7601; c) F. Kleitz, F. Bérubé, R. Guillet-Nicolas, C.-M. Yang, M. Thommes, *J. Phys. Chem. C* **2010**, *114*, 9344; d) H. Tuysuz, C. W. Lehmann, H. Bongard, B. Tesche, R. Schmidt, F. Schuth, *J. Am. Chem. Soc.* **2008**, *130*, 11510.

[22] a) E. P. Horwitz, D. R. McAlister, A. H. Bond, R. E. Barrans Jr, *Solv. Extract. Ion Exch.* **2005**, *23*, 319; b) Y. Lin, S. K. Fiskum, W. Yantasee, H. Wu, S. V. Mattigod, E. Vorpagel, G. E. Fryxell, *Environ. Sci. Technol.* **2005**, *39*, 1332.
[23] C. E. Fowler, S. L. Burkett, S. Mann, *Chem. Commun.* **1997**, 1769.
[24] S. Antonijevic, N. Halpern-Manners, *Solid State Nucl. Mag. Res.* **2008**, *33*, 82.
[25] G. P. Wang, T. C. Chang, Y. S. Hong, Y. S. Chiu, *Polymer* **2002**, *43*, 2191.
[26] S. Guan, S. Inagaki, T. Ohsuna, O. Terasaki, *Microporous Mesoporous Mater.* **2001**, *44–45*, 165.
[27] T. Azaïs, G. Hartmeyer, S. Quignard, G. Laurent, C. Tourné-Péteilh, J.-M. Devoisselle, F. Babonneau, *Pure Appl. Chem.* **2009**, *81*, 1345.
[28] L. Du, S. Liao, H. A. Khatib, J. F. Stoddart, J. I. Zink, *J. Am. Chem. Soc.* **2009**, *131*, 15136.
[29] J. D. Lunn, D. F. Shantz, *Chem. Mater.* **2009**, *21*, 3638.
[30] M. S. Killian, J.-F. Gnichwitz, A. Hirsch, P. Schmuki, J. Kunze, *Langmuir* **2010**, *26*, 3531.
[31] S. S. Jedlicka, J. L. Rickus, D. Y. Zemlyanov, *J. Phys. Chem. B.* **2007**, *111*, 11850.
[32] D. T. Pierce, J. X. Zhao, Trace Analysis with Nanomaterials, Wiley-VCH, Germany **2010**, p. 191.
[33] G. E. Fryxell, Y. Lin, S. Fiskum, J. C. Birnbaum, H. Wu, K. Kemner, S. Kelly, *Environ. Sci. Techol.* **2005**, *39*, 1324.
[34] S. A. Cotton, Lanthanide and Actinide Chemistry, John Wiley & Sons, Ltd., West Sussex, England **2006**.
[35] Y. Sasaki, G. R. Choppin, *J. Radioanal. Nucl. Chem.* **2000**, *246*, 267.
[36] a) N. V. Reichhardt, R. Guillet-Nicolas, M. Thommes, B. Klösgen, T. Nylander, F. Kleitz, V. Alfredsson, *Phys. Chem. Chem. Phys.* **2012**, *14*, 5651; b) H. Staub, R. Guillet-Nicolas, N. Even, L. Kayser, F. Kleitz, F.-G. Fontaine, *Chem. Eur. J.* **2011**, *17*, 4254.